Research Square

Preprints are preliminary reports that have not undergone peer review.
They should not be considered conclusive, used to inform clinical practice,
or referenced by the media as validated information.

PVN CRF/CRF-R1 signaling links stress to bowel dysfunction, anxiety-like behavior, and colonic barrier injury and is modulated by electroacupuncture in IBS-D-like mice

Guoming Shen

shengm64@ahtcm.edu.cn

Anhui University of Chinese Medicine https://orcid.org/0000-0002-5983-0370

Shun Huang
Chuqiao Shen
Chen Xu
Xiyang Wang
Jiangang Xu
Nannan Tian
Kan Ding
Hao Wang

Article

Keywords: Electroacupuncture, Irritable Bowel Syndrome, Corticotropin-Releasing Factor, Paraventricular Hypothalamic Nucleus, Intestinal Permeability

Posted Date: July 20th, 2026

DOI: https://doi.org/10.21203/rs.3.rs-10159491/v1

License: This work is licensed under a Creative Commons Attribution 4.0 International License.
Read Full License

Additional Declarations: The authors have declared there is **NO** conflict of interest to disclose

Abstract

Background

Diarrhea-predominant irritable bowel syndrome (IBS-D) is frequently accompanied by anxiety and intestinal barrier dysfunction, yet the central mechanisms linking stress-related neural signaling to peripheral colonic injury remain incompletely understood.

Aims

To investigate whether paraventricular hypothalamic nucleus (PVN) CRF/CRF-R1 signaling acts upstream of colonic barrier dysfunction and whether electroacupuncture (EA) alleviates IBS-D-like and anxiety-like phenotypes by modulating this pathway.

Methods

An IBS-D-like mouse model with anxiety-like behaviors was established by combining chronic restraint stress with intermittent chemical stimulation. Visceral sensitivity, bowel dysfunction, and anxiety-like behaviors were assessed. PVN CRF signaling was bidirectionally manipulated by stereotactic microinjection, and downstream changes in colonic CRF/CRF-R1 signaling, mast cell activation, inflammatory signaling, tight junction-related proteins, and permeability-associated markers were evaluated.

Results

Model mice exhibited visceral hypersensitivity, diarrhea-like symptoms, anxiety-like behaviors, and colonic barrier impairment. EA improved both gastrointestinal and affective abnormalities and reduced PVN CRF/CRF-R1 overactivation. Intra-PVN CRF administration reproduced key bowel and behavioral abnormalities in otherwise normal mice, whereas CRF-R1 blockade alleviated these changes in model mice. Central manipulation of PVN CRF signaling was accompanied by corresponding alterations in colonic CRF/CRF-R1 expression, mast cell degranulation, TNF-α/NF-κB/MLCK signaling, tight junction-related proteins, and permeability-associated changes.

Conclusions

These findings support a PVN-driven brain–gut–barrier mechanism in which CRF/CRF-R1 signaling contributes to bowel dysfunction, anxiety-like behavior, and colonic barrier injury in IBS-D-like mice. EA alleviated these abnormalities, at least in part, through modulation of this pathway.

1. Introduction

Irritable bowel syndrome (IBS) is a common disorder of gut-brain interaction characterized by recurrent abdominal pain associated with altered bowel habits [1–4]. Among its subtypes, diarrhoea-predominant

IBS (IBS-D) is particularly prevalent and is associated with substantial impairment in quality of life and a considerable socioeconomic burden[1, 2]. In addition to bowel symptoms, IBS frequently co-occurs with psychiatric disorders, especially anxiety and depression [5]. In IBS-D with emotional comorbidity, gastrointestinal dysfunction and affective disturbances often coexist, suggesting coordinated dysregulation along the brain-gut axis. Although the pathogenesis of IBS is multifactorial, epithelial barrier dysfunction is increasingly recognized as an important pathological feature, together with visceral hypersensitivity and low-grade mucosal inflammation [6, 7]. Current treatments, including dietary interventions, fecal microbiota transplantation, antispasmodics, neuromodulators, and probiotics, aim to relieve both gastrointestinal and psychological symptoms [8–10]. However, their efficacy remains variable, highlighting the need for more effective mechanism-based therapies.

Stress-related corticotropin-releasing factor (CRF) signaling is considered a potential driver of brain-gut dysregulation in IBS [11–18]. CRF is a key mediator of the stress response and is distributed in both the central nervous system and peripheral tissues, including the gastrointestinal tract. In patients with IBS-D, elevated CRF levels are positively associated with symptom severity and the extent of anxiety and depression[19–21]. Mechanistically, CRF has been linked to mast cell activation, chronic intestinal inflammation, visceral hypersensitivity, and impairment of mucosal barrier integrity[12–14]. These observations suggest that stress-related CRF signaling may provide an important molecular link between central stress responses and peripheral intestinal barrier injury in IBS-D.

The paraventricular nucleus (PVN) of the hypothalamus is a critical autonomic and neuroendocrine integration center that plays an important role in the regulation of gastrointestinal function [22, 23]. As a major hypothalamic source of CRF, the PVN is well positioned to translate stress-related signals into downstream gastrointestinal responses [24]. Previous studies have shown that CRF neurons are involved in stress-induced gastric dysfunction [18], supporting the importance of central CRF pathways in stress-related gastrointestinal regulation. Nevertheless, it remains unclear whether CRF/CRF receptor 1 (CRF-R1) signaling within the PVN lies upstream of colonic barrier injury and permeability-related alterations in IBS-D with emotional comorbidity.

Electroacupuncture (EA) has been reported to improve gastrointestinal symptoms and emotional disturbances in disorders of gut-brain interaction [25–30]. On this basis, EA may represent a potential intervention capable of interrupting stress-related CRF signaling along the brain-gut pathway. Therefore, the present study focused on PVN CRF/CRF-R1 signaling and the peripheral colonic CRF-related pathway to determine whether central CRF signaling contributes to IBS-D-like and anxiety-like phenotypes by promoting colonic neuroimmune activation, barrier injury, and permeability-related alterations, and whether EA can ameliorate these abnormalities by suppressing this pathway. By addressing these questions, this study sought to clarify whether PVN CRF/CRF-R1 signaling functions upstream of colonic barrier dysfunction and to provide experimental evidence for a PVN-driven brain-gut-barrier mechanism in IBS-D with emotional comorbidity.

2. Materials and methods

2.1 Animals

Male C57BL/6J mice (8–10 weeks old) were obtained from Hangzhou Ziyuan Experimental Animal Science and Technology Co., Ltd. Mice were housed (six per cage) under controlled conditions (12 h light/dark cycle, 23–25°C, 50% humidity) with ad libitum access to food and water, except where specified. All procedures were approved by the Animal Experimentation Ethics Committee of Anhui University of Chinese Medicine (Approval No. AHUCM-mouse-2024148) and were conducted in accordance with relevant animal welfare regulations and the ARRIVE guidelines.

Animals were allocated to experimental groups using a randomized procedure.

Blinding: Investigators conducting behavioral testing and outcome assessments, as well as those performing statistical analyses, were blinded to group allocation until completion of data analysis.

2.2 Reagents

Isoflurane (#R510-22-10) was purchased from RWD Company; acetic acid (#10000218) from Sinopharm Chemical Reagent Co., Ltd.; CRF (#TRC-C695750) from LGC Company; and Antalarmin (#HY-124457) from MCE Company. The following antibodies were obtained from ZENBIO Biotechnology Co., Ltd.: CRF primary antibody (#860209), CRFR1 monoclonal antibody (#370069), NF-κB P65 monoclonal antibody (#380172), Myosin light chain kinase (MLCK) monoclonal antibody (#R381015); The TNF-α monoclonal antibody (#60291-1-Ig) was obtained from Proteintech Biotechnology CO. HRP-conjugated goat anti-rabbit secondary antibody (#ZB-2301) and HRP-conjugated goat anti-mouse secondary antibody (#ZB-2305, ACTIN (#TA-09)) were purchased from Zs-BIO Co., Ltd.;The prestained protein marker (#26617) was obtained from Thermofish; ZO-1 monoclonal antibody (#21773-1-AP), Occludin monoclonal antibody (#27260-1-AP), and Claudin-1 primary antibody (#13050-1-AP); Hematoxylin-eosin stain (#G1005), toluidine blue stain (#G1032), electron microscope fixative (#G1102), BCA protein quantitative detection kit (#G2026-200T), ultrasensitive ECL chemiluminescence kit (#G2020-25ML), bovine serum albumin (BSA) (#GC305010), DAPI staining reagent (#G1012), and anti-fluorescence quenching blocking tablets (#G1401) were purchased from Servicebio. The diamine oxidase (DAO) kit (#JL-T2400-48 samples), mouse interleukin 1β (IL-1β) ELISA kit (#JL18442-96T), mouse interleukin 6 (IL-6) ELISA kit (#JL20268-96T), and mouse TNF-α ELISA kit (#JL10484-96T) were obtained from Jianglai Biologicals.

2.3 Experimental models and evaluation

To recapitulate the comorbidity of IBS-D and emotional disturbance observed in patients, we established a mouse model using a protocol adapted from previous reports with modifications [31, 32]. This composite model integrates chronic psychological restraint stress and intermittent colonic chemical irritation.

Briefly, mice were individually restrained in ventilated 50 mL conical tubes (with the plunger fixed at the 40 mL mark) for 3 h per session, twice daily, over 28 consecutive days. To enhance visceral sensitivity,

intrarectal administration of 3% acetic acid (150 μL) was performed every other day from day 22 onward. Age-matched control mice were housed under standard conditions without any intervention.

Model validity was assessed at the endpoint by visceral sensitivity (AWR during colorectal distension), bowel function (diarrhea index), and anxiety-like behaviors (reduced open-arm exploration in the elevated plus maze and reduced center activity in the open field test).

2.4 Electroacupuncture stimulation

Electroacupuncture was delivered once daily for 20 min for 7 consecutive days using a disperse–dense waveform (Hua Tuo SDZ-IV; Suzhou Medical Supplies Factory Co., Ltd.). Stimulation was set at 0.5 mA and 2/10 Hz. Sterile disposable needles (0.25 × 13 mm) were inserted at ST25 (bilateral; 5 mm lateral to the umbilicus), BL25 (bilateral; 5 mm lateral to the L4 spinous process), and GV20 (midline at the vertex). Mice were anesthetized with isoflurane (3% induction; 0.5%–1% maintenance).

2.5 Evaluation of visceral sensitivity

Visceral sensitivity was assessed using the abdominal withdrawal reflex (AWR) during colorectal distension (CRD). Mice were fasted for 12 h before testing. A lubricated balloon catheter was inserted 0.5 cm into the colorectum. After a 15 min acclimation period, the balloon was inflated stepwise to 20, 40, 60, and 80 mmHg for 20 s, with a 4 min inter-stimulus interval between distensions. AWR scores were independently rated by two observers blinded to group allocation, and the mean of three measurements was recorded. AWR scoring criteria were: 0, no response; 1, brief head movement/occasional writhing; 2, mild abdominal muscle contraction; 3, clear abdominal contraction with abdominal lifting; 4, strong contraction with body arching and pelvic lifting.

2.6 Determination of diarrhea index

Clean, dry trays lined with fresh filter paper (changed hourly) were used for stool collection. Over a 6 h period, the total number of fecal pellets, the number of loose stools, and the diameter of each loose stool were recorded by two independent investigators. The diarrhea index was calculated as follows:

Diarrhea index = dilute stool rate × average dilute stool grade

Dilute stool rate = number of dilute stools/total number of stools

Average dilute stool grade = sum of all dilute stool grades/number of dilute stools

Dilute stool grades were classified based on stool diameter:

< 1 cm = grade 1; 1-1.9 cm = grade 2; 2–3 cm = grade 3; and 3 cm = grade 4.

If feces could not be separated into discrete pellets, the default was recorded as one pile equaling one pellet.

2.7 Behavioural experiments

2.7.1 OFT

Mice were placed in the peripheral zone of the OFT arena (RWD Life Science Co., Ltd., China). The open field apparatus consisted of a square arena (100 cm × 100 cm × 50 cm, length × width × height). Following a 30 s acclimatization period, locomotor activity and anxiety-like behavior were recorded for 5 min and analyzed using SMART v3.0, including total distance traveled, distance traveled in the center zone, and time spent in the center zone.

Center-zone definition: The center zone was defined in SMART v3.0 as the central region of the arena, with boundaries set identically for all animals prior to analysis.

2.7.2 EPM

The elevated plus (RWD Life Science Co., Ltd., China) maze consisted of two open arms and two closed arms (arm length 35 cm, arm width 5 cm) connected by a central platform (5 cm × 5 cm). The closed arms were surrounded by 15 cm-high walls. The maze was elevated 40–55 cm above the floor. Mice were acclimated in a quiet environment for 30 min before testing, after which they were placed at the center facing an open arm. Behavior was recorded for 5 min and analyzed using SMART v3.0; the number of open-arm entries and time spent in the open arms were quantified. The apparatus was cleaned with 70% ethanol between animals.

2.8 Intracerebral cannula drug delivery

Mice were anesthetized and placed in a stereotaxic frame (RWD, #68803) on a heating pad (36°C). Bilateral guide cannulae were implanted targeting the PVN using the following coordinates relative to bregma: AP − 0.62 mm, ML ± 0.25 mm, DV − 4.55 mm. After 7 days of recovery, drugs were infused bilaterally (0.5 μL per side over 5 min), and the injector was left in place for an additional 5 min to minimize backflow. Postoperative analgesia was not administered, as it was considered to potentially interfere with neurobehavioral assessments. Animals were closely monitored during postoperative recovery and throughout the 7-day recovery period for general condition, activity, grooming, and wound status. No adverse events were observed.

Animals with cannula placements outside the PVN, unilateral misplacement, or obvious tissue damage along the injection track were excluded from the final analysis. No additional exclusion criteria were applied.

2.9 Preparation of CRF-R1 antagonist

Antalarmin (CRF-R1 antagonist, #HY-124457, MCE) was prepared by dissolving 5 mg of Antalarmin in 0.5 mL of dimethyl sulfoxide (DMSO) with vortexing until fully dissolved to yield a 10 mg/mL stock solution. To prepare the working solution, 25 μL of the stock solution was diluted with 975 μL of sterile saline to obtain a final 0.25 mg/mL concentration. For bilateral intra-PVN infusion, 0.5 μL was delivered per side, corresponding to 125 ng per side. Aliquots were stored in sterile Eppendorf tubes (EP tubes) at − 20°C, protected from light, and used without repeated freeze-thaw cycles.

2.10 Preparation of CRF solution

CRF (1 mg) was dissolved in 1 mL of sterile phosphate-buffered saline (PBS) at pH 7.4 with gentle vortexing. For bilateral intra-PVN infusion, 0.5 μL was delivered per side, corresponding to 0.5 μg per side. The solution was filtered using a 0.22 μm sterile filter, aliquoted into sterile EP tubes, and stored at − 80°C.

2.11 Western blot assay

Colon tissue proteins were extracted and quantified. Protein samples were subjected to SDS-PAGE and transferred to PVDF membranes *via* wet transfer. After incubation with primary antibodies, membranes were washed and incubated with HRP-conjugated goat anti-rabbit IgG (1:5000, GB23303, Servicebio) at room temperature (RT). Detection was performed using a chemiluminescent substrate, and images were captured using a Tanon 5200 imaging system. The relative protein expression levels were normalized to β-actin and quantified using ImageJ software (version 1.54f).

2.12 Immunofluorescence (IF)

Mouse colon tissues were paraffin-embedded and sectioned at 5 μm thickness, while brain tissues were cryosectioned at 40 μm. Tissue sections were washed with PBS for 5 min × 3 times, followed by blocking with 0.5% Triton X-100 and 5% BSA at RT for 1 h. Subsequently, sections were incubated at 4°C for 16 h with primary antibody in a solution containing 0.3% Triton X-100, 3% BSA, and 3% donkey serum. After incubation, sections were washed with PBS (5 min × 3 times), followed by incubation at RT, protected from light, for 2 h with the corresponding secondary antibody. After washing again with PBS (5 min × 3 times), the sections were mounted and observed using a fluorescence microscope (LEICA DM 2500 LED). Quantitative analysis of fluorescence intensity was performed using ImageJ software (version 1.54f).

2.13 Enzyme-linked immunosorbent assay (ELISA)

Blood was collected from the abdominal aorta of mice and left at RT for 1 h, then centrifuged at 3000 ×g for 15 min to separate the serum. The supernatant was collected and stored at 4°C. All ELISA procedures were performed according to the manufacturer's protocols and analyzed using an enzyme-linked immunosorbent analyzer (RT-6100, Rayto). A standard curve was generated by plotting standard concentrations against their corresponding absorbance values.

2.14 Hematoxylin and eosin (HE) and toluidine blue staining

Colon tissues were fixed in 4% paraformaldehyde for 24 h, dehydrated through a graded ethanol series, embedded in paraffin, and sectioned at 5 μm thickness. Sections were floated on a 42°C water bath to facilitate expansion, carefully transferred onto adhesive-coated slides, and flattened using a histological brush to remove wrinkles. Slides were then dried in a 60°C slide dryer for 1 h. For HE staining, sections after staining were differentiated with acid alcohol and mounted with neutral gum. Microscopic

observations were made using a LEICA DM 2500 LED microscope. For toluidine blue staining, after dehydration, embedding, sectioning, and deparaffinization, sections were stained with toluidine blue solution, differentiated with glacial acetic acid until nuclei and granules were clearly defined, and mounted with neutral gum. MC degranulation in the intestinal mucosa was microscopically observed, with MCs identified as round, oval, or irregular in shape.

2.15 Transmission electron microscopy of colonic mucosal ultrastructure

Mouse colon tissues were trimmed into ~ 1 mm³ blocks, rinsed in pre-cooled PBS (3 × min), dehydrated through graded ethanol, processed according to standard TEM procedures, and imaged using a transmission electron microscope (Hitachi HT7800).

2.16 Statistical analysis

Statistical analyses were performed using SPSS 25.0, and data visualization using GraphPad Prism 9. Data are expressed as mean ± standard deviation (mean ± SD). For comparisons between two groups, unpaired *t*-tests were used when data met the assumptions of normal distribution. One-way ANOVA was applied for comparisons among multiple groups, followed by Tukey's test for post hoc analysis when variance was homogeneous; otherwise, Dunnett's T3 test was employed. When normality or homogeneity of variance was not satisfied, the Kruskal–Wallis test was used. A P value < 0.05 was considered statistically significant. No formal sample size calculation was performed; sample sizes were based on previous experience and common practice in similar animal studies.

3. Results

3.1 Electroacupuncture alleviates visceral hypersensitivity, intestinal dysfunction, and anxiety-like behaviors in mice model of IBS-D with emotional comorbidity

To evaluate the therapeutic effects of electroacupuncture (EA), we established a mouse model of IBS-D with emotional comorbidity using chronic restraint stress combined with chemical stimulation (Fig. 1A, B). We first assessed model establishment by comparing the Model group with the Control group. Compared with the Control group, mice in the Model group showed significant weight loss (P < 0.001; Fig. 1C), together with marked visceral hypersensitivity and intestinal dysfunction, as reflected by a reduced visceral pain threshold, increased fecal water content, and higher diarrhea index scores (P < 0.001; Fig. 1D–F). Behavioral tests further indicated the presence of anxiety-like changes in the Model group. In the elevated plus maze (EPM), Model mice showed a lower percentage of open-arm entries than Control mice (P < 0.001; Fig. 1G, H). In the open field test (OFT), they also exhibited reduced total distance traveled, reduced distance traveled in the center zone, and less time spent in the center zone (P < 0.05, P < 0.01; Fig. 1I–L). Together, these findings indicate that the IBS-D model with emotional comorbidity was successfully established.

We next examined the effects of EA on these abnormalities. Compared with the Model group, EA-treated mice showed increased body weight and visceral pain thresholds, along with reduced fecal water content and diarrhea index scores ($P < 0.01$, $P < 0.001$; Fig. 1C–F). EA also attenuated anxiety-like changes. In the EPM, EA increased the percentage of open-arm entries ($P < 0.01$; Fig. 1G, H). In the OFT, EA-treated mice showed increases in total distance traveled, center distance, and center time ($P < 0.05$; Fig. 1I–L). These results indicate that EA ameliorates both intestinal dysfunction and anxiety-like behaviors in this comorbid IBS-D model.

Histological examination of the distal colon provided further support for these findings (Fig. 1M). In the Control group, the colonic mucosa was intact, with well-organized crypt architecture and no obvious inflammatory cell infiltration. In contrast, the Model group showed disrupted mucosal architecture and irregular glandular arrangement, accompanied by inflammatory cell infiltration in the mucosa and submucosa. EA treatment partially restored mucosal structure, with a more regular glandular arrangement and reduced inflammatory cell infiltration compared with the Model group.

Given that EA improved both intestinal dysfunction and anxiety-like behaviors in this comorbid model, we next investigated whether these effects were associated with alterations in the PVN CRF/CRF-R1 signaling pathway.

3.2 Electroacupuncture suppresses CRF and CRF-R1 protein expression in the hypothalamic PVN of IBS-D mice with emotional comorbidity

The hypothalamic PVN is a key brain region involved in stress responses and anxiety regulation, and has been implicated in stress-related gastrointestinal dysfunction [33]. To determine whether PVN CRF/CRF-R1 signaling is altered in IBS-D with emotional comorbidity, we first examined CRF and CRF-R1 protein expression in the PVN. Compared with the Control group, mice in the Model group showed significantly increased protein levels of both CRF and CRF-R1 in the PVN ($P < 0.001$; Fig. 2A, B). Immunofluorescence staining further supported these findings, showing higher mean fluorescence intensities of CRF and CRF-R1 in the Model group than in the Control group ($P < 0.01$, $P < 0.001$; Fig. 2C, D). These results indicate that PVN CRF/CRF-R1 signaling is upregulated in IBS-D mice with emotional comorbidity.

We next examined whether EA modulated these molecular changes. Compared with the Model group, EA treatment significantly reduced CRF and CRF-R1 protein expression in the PVN ($P < 0.001$, $P < 0.01$; Fig. 2A, B). Consistently, the mean fluorescence intensities of CRF and CRF-R1 were also decreased in the EA group ($P < 0.05$, $P < 0.001$; Fig. 2C, D). These findings suggest that PVN CRF/CRF-R1 signaling may contribute to the comorbid phenotype and represent a potential central target of EA intervention.

3.3 Activation of PVN CRF signaling induces IBS-D-like and anxiety-like phenotypes that are attenuated by electroacupuncture

To determine whether activation of PVN CRF signaling is sufficient to induce bowel and affective abnormalities, we performed bilateral microinjection of CRF into the PVN of control mice and then examined whether EA could attenuate the resulting phenotypes, as shown in the experimental timeline and schematic (Fig. 3A, B). Compared with the Control (Vehicle) group, intra-PVN CRF microinjection induced significant visceral hypersensitivity ($P < 0.001$; Fig. 3C) and intestinal dysfunction, as reflected by increased fecal water content and higher diarrhea index scores ($P < 0.001$; Fig. 3D, E). In addition, CRF microinjection elicited anxiety-like changes, as indicated by a lower percentage of open-arm entries in the elevated plus maze (EPM) ($P < 0.01$; Fig. 3F, G) and reduced total distance traveled, center distance, and center time in the open field test (OFT) ($P < 0.01$, $P < 0.001$; Fig. 3H–K). These results indicate that activation of PVN CRF signaling is sufficient to recapitulate key IBS-D-like and anxiety-like phenotypes in otherwise normal mice.

We next examined whether EA could mitigate these CRF-induced abnormalities. Compared with the CRF group, the CRF + EA group showed a higher visceral pain threshold ($P < 0.05$; Fig. 3C), together with reduced fecal water content and lower diarrhea index scores ($P < 0.001$, $P < 0.01$; Fig. 3D, E). EA also attenuated anxiety-like changes, as evidenced by an increased percentage of open-arm entries in the EPM ($P < 0.01$; Fig. 3F, G) and increases in total distance traveled, center distance, and center time in the OFT ($P < 0.05$, $P < 0.01$; Fig. 3H–K). These findings indicate that activation of PVN CRF signaling is sufficient to induce key IBS-D-like and anxiety-like phenotypes, and that EA partially counteracts these CRF-driven abnormalities.

3.4 Blockade of PVN CRF-R1 signaling alleviates IBS-D-like and anxiety-like phenotypes in comorbidity model mice

To complement the gain-of-function experiment above, we next tested whether pharmacologic blockade of PVN CRF-R1 signaling could alleviate established bowel and affective abnormalities in the comorbidity model. To this end, the selective CRF-R1 antagonist antalarmin was bilaterally administered into the PVN of model mice (Fig. 4A, B). Compared with the vehicle-treated Model group, intra-PVN administration of antalarmin significantly alleviated visceral hypersensitivity ($P < 0.01$; Fig. 4C) and improved intestinal dysfunction, as indicated by reduced fecal water content and lower diarrhea index scores ($P < 0.05$, $P < 0.01$; Fig. 4D, E). Antalarmin also attenuated anxiety-like changes, as shown by an increased percentage of open-arm entries in the EPM ($P < 0.05$; Fig. 4F, G) and increases in total distance traveled, center distance, and center time in the OFT ($P < 0.01$; Fig. 4H–K). These findings indicate that PVN CRF-R1 signaling functionally contributes to the bowel and affective abnormalities of the comorbidity model.

Together with the CRF microinjection results, these findings support a causal contribution of PVN CRF/CRF-R1 signaling to the somatic and emotional phenotypes of the comorbidity model.

3.5 PVN CRF signaling regulates peripheral colonic CRF/CRF-R1 expression

To determine whether central PVN CRF signaling is associated with changes in the peripheral colonic CRF system, we first examined colonic CRF and CRF-R1 expression after intra-PVN CRF microinjection. Western blot analysis showed that intra-PVN CRF microinjection significantly increased colonic CRF and CRF-R1 protein levels compared with the Control group ($P < 0.001$; Fig. 5A). Immunofluorescence staining of the distal colon further showed increased CRF fluorescence intensity in the CRF group ($P < 0.001$; Fig. 5B). We next examined whether EA could attenuate these CRF-induced colonic changes. Compared with the CRF group, EA treatment significantly reduced colonic CRF and CRF-R1 protein expression ($P < 0.001$; Fig. 5A) and decreased CRF fluorescence intensity in the distal colon ($P < 0.01$; Fig. 5B). These findings indicate that activation of PVN CRF signaling is associated with enhanced peripheral colonic CRF system expression, which can be attenuated by EA.

To complement the gain-of-function experiment above, we next examined whether blockade of central CRF-R1 signaling would reverse colonic CRF system abnormalities in the comorbidity model. Western blot analysis showed that intra-PVN administration of the CRF-R1 antagonist antalarmin significantly reduced colonic CRF and CRF-R1 protein expression compared with the vehicle-treated Model group ($P < 0.01$, $P < 0.001$; Fig. 5C). Consistently, immunofluorescence analysis showed that antalarmin significantly decreased CRF fluorescence intensity in the distal colon ($P < 0.01$; Fig. 5D). Together, these findings indicate that PVN CRF/CRF-R1 signaling is associated with peripheral colonic CRF system expression.

These findings support the presence of a functional PVN-colonic CRF signaling axis linking central stress signaling to peripheral colonic responses.

3.6 Electroacupuncture attenuates colonic mast cell activation and the downstream TNF-α/NF-κB/MLCK inflammatory pathway

To determine whether EA modulates downstream colonic neuroimmune activation, we first examined mast cell activation in the distal colon. Toluidine blue staining showed that the mast cell degranulation rate was significantly higher in the Model group than in the Control group ($P < 0.001$; Fig. 6A). Consistently, immunofluorescence analysis showed increased fluorescence intensity of mast cell tryptase (MCT), a marker of mast cell activation, in the Model group ($P < 0.001$; Fig. 6B). These findings indicate that mast cell activation is enhanced in the colon of comorbidity model mice.

We next examined downstream inflammatory signaling in colonic tissue. Western blot analysis showed that the protein levels of CRF, CRF-R1, TNF-α, NF-κB p65, and MLCK were all significantly increased in the Model group compared with the Control group ($P < 0.001$; Fig. 6C). In addition, ELISA showed that serum levels of the pro-inflammatory cytokines TNF-α, IL-1β, and IL-6 were significantly elevated in the Model group ($P < 0.001$; Fig. 6D–F). These results indicate that colonic mast cell activation is accompanied by upregulation of downstream inflammatory signaling in the comorbidity model.

We next assessed the effects of EA on these changes. Compared with the Model group, EA treatment significantly reduced both the mast cell degranulation rate and MCT fluorescence intensity in the distal

colon ($P < 0.01$; Fig. 6A, B). EA also significantly decreased the colonic protein expression of CRF, CRF-R1, TNF-α, NF-κB p65, and MLCK ($P < 0.001$; Fig. 6C), together with reduced serum levels of TNF-α, IL-1β, and IL-6 ($P < 0.001$; Fig. 6D–F). These findings suggest that EA attenuates CRF-related mast cell-inflammatory signaling in the colon, thereby providing a mechanistic link between central stress dysregulation and peripheral mucosal injury.

3.7 Electroacupuncture restores colonic barrier integrity and ameliorates permeability-related alterations

To assess colonic barrier integrity, we first examined the expression of tight junction (TJ) proteins in the distal colon. Immunofluorescence analysis showed that the fluorescence intensities of Claudin-1, ZO-1, and Occludin were significantly reduced in the Model group compared with the Control group ($P < 0.05$, $P < 0.001$; Fig. 7A–F). These findings indicate that barrier-associated TJ proteins are downregulated in the comorbidity model.

We next examined epithelial ultrastructure by transmission electron microscopy (TEM). In the Model group, the colonic epithelium showed sparse, disorganized, and shortened microvilli, together with disrupted tight junctions and widened intercellular spaces (Fig. 7G). In addition, serum levels of diamine oxidase (DAO), a marker associated with intestinal permeability, were significantly elevated in the Model group compared with the Control group ($P < 0.01$; Fig. 7H). Together, these results indicate that the comorbidity model is accompanied by colonic barrier disruption and permeability-related alterations.

We next assessed whether EA could reverse these abnormalities. Compared with the Model group, EA treatment significantly increased the fluorescence intensities of Claudin-1, ZO-1, and Occludin ($P < 0.05$, $P < 0.01$; Fig. 7A–F). TEM further showed that EA improved mucosal ultrastructure, with denser and more regularly arranged microvilli, together with better-preserved tight junctions and intercellular architecture (Fig. 7G). In addition, EA significantly reduced serum DAO levels compared with the Model group ($P < 0.05$; Fig. 7H). Collectively, these data indicate that EA is associated with restoration of colonic barrier integrity and improvement of permeability-related changes, which is consistent with suppression of the PVN-driven brain-gut-barrier axis.

4. Discussion

Chronic stress is a major contributor to disorders of gut-brain interaction and is closely linked to the coexistence of bowel dysfunction and affective symptoms in IBS-D [34]. In the present study, mice exposed to chronic restraint stress combined with chemical stimulation developed visceral hypersensitivity, diarrhea-like manifestations, anxiety-like behaviors, low-grade mucosal inflammatory changes, and evidence of colonic barrier impairment, supporting the suitability of this model for studying stress-related IBS-D-like pathology [31, 32, 35–37]. We further found that CRF and CRF-R1 expression in the PVN was significantly increased in model mice, that intra-PVN CRF administration reproduced key somatic and emotional abnormalities, and that intra-PVN CRF-R1 blockade alleviated these changes. In

parallel, EA improved both central and peripheral abnormalities, including behavioral changes, colonic inflammatory activation, and barrier-related injury. Together, these findings support the involvement of PVN CRF/CRF-R1 signaling in the comorbid phenotype and indicate that EA exerts a broad modulatory effect on this stress-related pathological process.

A key finding of the present study is that the significance of PVN CRF/CRF-R1 signaling may extend beyond symptom regulation to an upstream role in colonic barrier dysfunction in IBS-D with emotional comorbidity. Previous work has linked CRF signaling to stress-related gastrointestinal dysfunction and to mast cell-associated mucosal abnormalities[17–19, 22, 38–41]. However, whether CRF/CRF-R1 signaling within the PVN lies upstream of colonic barrier injury and permeability-related changes has remained unclear. In the present study, PVN CRF activation induced bowel and affective abnormalities together with enhanced colonic CRF signaling, whereas CRF-R1 blockade and EA both attenuated these changes. These results support the view that PVN CRF/CRF-R1 signaling is not merely associated with IBS-D-like pathology, but may function as an upstream regulator linking stress-related central dysfunction to peripheral colonic injury.

The PVN is a major hypothalamic center integrating neuroendocrine and autonomic stress responses and influencing gastrointestinal function [22, 42, 43]. CRF, as a principal mediator of the stress response, regulates both emotional and visceral processes through CRF receptors [44–48]. Consistent with previous studies showing that CRF-R1 preferentially mediates stress-induced colonic hypermotility and visceral hypersensitivity [38, 40, 43, 49–52], our results showed that PVN CRF/CRF-R1 signaling was upregulated in model mice and that gain- and loss-of-function manipulation of this pathway bidirectionally regulated IBS-D-like and anxiety-like phenotypes. Notably, central manipulation of PVN CRF signaling also altered colonic CRF and CRF-R1 expression, suggesting the presence of a functional top-down pathway linking hypothalamic stress signaling to the peripheral CRF system. Although the precise descending routes were not examined here, these findings support a PVN-colonic CRF signaling axis that may transmit stress-related central signals to the gut.

At the peripheral level, our findings support a pathway in which enhanced colonic CRF signaling is accompanied by mast cell activation, inflammatory signaling, and barrier disruption. Peripheral CRF and its receptors are widely distributed in the gastrointestinal tract [53–58], and CRF-R1 activation has been implicated in mast cell degranulation, intestinal inflammation, visceral hypersensitivity, and barrier impairment [59–62]. In line with this framework, model mice in the present study showed increased mast cell degranulation, upregulation of CRF, CRF-R1, TNF-α, NF-κB p65, and MLCK, elevated circulating inflammatory cytokines, reduced expression of Claudin-1, ZO-1, and Occludin, ultrastructural disruption of tight junctions, and increased serum diamine oxidase (DAO). These findings are consistent with the notion that mast cell-associated inflammatory activation contributes to disruption of epithelial junctional integrity and permeability-related alterations [63–74]. Thus, our data support a peripheral CRF-mast cell-inflammatory-barrier cascade as an important downstream effector pathway in this comorbidity model.

Acupuncture has been increasingly recognized as a non-pharmacological intervention for functional gastrointestinal disorders, and the acupoint combination used here was selected on the basis of previous studies and our prior work[18, 24, 25, 46, 75–79]. In the present study, EA reduced PVN CRF/CRF-R1 overactivity, attenuated CRF-driven bowel and affective abnormalities, suppressed colonic mast cell-inflammatory activation, and improved barrier-related changes. These effects suggest that EA may mitigate IBS-D-like pathology with emotional comorbidity by modulating stress-related central-peripheral signaling rather than acting only at a single peripheral target.

Several limitations should be acknowledged. First, we did not perform double-label immunofluorescence in this cohort to directly visualize CRF-R1 localization on colonic mast cells, although our previous work [24] provides relevant structural support. Second, while our findings implicate the PVN as a key upstream hub, the specific autonomic pathways transmitting PVN CRF signals to the colon were not identified. Third, sham EA and non-acupoint controls were not included, which limits assessment of acupoint specificity. Fourth, although the present data support a pathway linking PVN CRF/CRF-R1 signaling to peripheral barrier-related injury, some mechanistic links remain inferential and will require further validation using pathway-specific or cell-specific approaches. Future studies combining neural circuit tracing, targeted pathway manipulation, and cell-type-resolved analyses will help refine the brain-gut-barrier mechanism proposed here.

Conclusion

In summary, the present study supports a PVN-driven brain–gut–barrier mechanism in IBS-D with emotional comorbidity. Chronic stress was associated with activation of PVN CRF/CRF-R1 signaling, which may contribute to bowel dysfunction, anxiety-like behavior, colonic neuroimmune activation, and barrier-related injury. Electroacupuncture attenuated these abnormalities in association with suppression of PVN CRF/CRF-R1 signaling and downstream mast cell–TNF-α/NF-κB/MLCK-related barrier disruption. These findings identify PVN CRF/CRF-R1 signaling as a potential upstream regulator of colonic barrier dysfunction and suggest that CRF-R1- and MLCK-related pathways may represent candidate mechanistic targets in IBS-D.

Declarations

Ethics approval and consent to participate

All animal experiments were approved by the Animal Experimentation Ethics Committee of Anhui University of Chinese Medicine (Approval No. AHUCM-mouse-2024148, Hefei, China) and were conducted in accordance with institutional guidelines and the ARRIVE guidelines.

Authorship contribution

Conceptualization: Guoming Shen, Hao Wang. Methodology: Chen Xu, Guoming Shen, Hao Wang. Investigation: Shun Huang, Jiangang Xu, Chuqiao Shen. Formal analysis: Chen Xu, Nannan Tan, Kan Ding. Supervision: Guoming Shen, Hao Wang. Writing – original draft: Shun Huang, Chuqiao Shen. Writing – review & editing: Guoming Shen, Chen Xu, Hao Wang. Technical support for stereotaxic surgery: Xi-Yang Wang. All authors read and approved the final manuscript.

Competing interests

The authors declare that they have no competing interests.

Funding

This work was supported by the Excellent Youth Project of Anhui Universities (No. 2022AH030065), the National Natural Science Foundation of China (No. 82474224), the Anhui Provincial Natural Science Foundation (No. 2408085MH223), the Open Project of Anhui Province Key Laboratory of Meridian–Viscera Correlationship (No. 2024AHMVC04), the Research Project of Xin'an Medical and Chinese Medicine Modernization Research Institute (No. 2023CXMMTCM016), and the Anhui University of Chinese Medicine Exploratory Research Project (No. AHUCM2024TS034).

Data availability statement

The data supporting the findings of this study are available from the corresponding authors upon reasonable request. Due to file size and data management constraints, full-length behavioral videos and certain raw image files are not publicly deposited.

References

1. Ford AC, Sperber AD, Corsetti M, Camilleri M. Irritable bowel syndrome. Lancet 2020;396:1675–1688.
2. Mayer EA, Ryu HJ, Bhatt RR. The neurobiology of irritable bowel syndrome. Mol Psychiatry 2023;28:1451–1465.
3. Black CJ, Ford AC. Global burden of irritable bowel syndrome: trends, predictions and risk factors. Nat Rev Gastroenterol Hepatol 2020;17:473–486.
4. Aziz MNM, Kumar J, Muhammad Nawawi KN, Raja Ali RA, Mokhtar NM. Irritable Bowel Syndrome, Depression, and Neurodegeneration: A Bidirectional Communication from Gut to Brain. Nutrients 2021;13.
5. Staudacher HM, Mikocka-Walus A, Ford AC. Common mental disorders in irritable bowel syndrome: pathophysiology, management, and considerations for future randomised controlled trials. Lancet Gastroenterol Hepatol 2021;6:401–410.

6. Huang KY, Wang FY, Lv M, Ma XX, Tang XD, Lv L. Irritable bowel syndrome: Epidemiology, overlap disorders, pathophysiology and treatment. World J Gastroenterol 2023;29:4120–4135.
7. Holtmann GJ, Ford AC, Talley NJ. Pathophysiology of irritable bowel syndrome. Lancet Gastroenterol Hepatol 2016;1:133–146.
8. Camilleri M. Diagnosis and Treatment of Irritable Bowel Syndrome: A Review. Jama 2021;325:865–877.
9. Reed B, Buzenski J, van Tilburg MAL. Implementing psychological therapies for gastrointestinal disorders in pediatrics. Expert Rev Gastroenterol Hepatol 2020;14:1061–1067.
10. Fikree A, Byrne P. Management of functional gastrointestinal disorders. Clin Med (Lond) 2021;21:44–52.
11. Jonassen AK, Wergeland A, Helgeland E, Mjøs OD, Brar BK. Activation of corticotropin releasing factor receptor type 2 in the heart by corticotropin releasing factor offers cytoprotection against ischemic injury via PKA and PKC dependent signaling. Regul Pept 2012;174:90–97.
12. Sinagra E, Pompei G, Tomasello G, et al. Inflammation in irritable bowel syndrome: Myth or new treatment target? World J Gastroenterol 2016;22:2242–2255.
13. De Winter BY, van den Wijngaard RM, de Jonge WJ. Intestinal mast cells in gut inflammation and motility disturbances. Biochim Biophys Acta 2012;1822:66–73.
14. D'Costa S, Ayyadurai S, Gibson AJ, et al. Mast cell corticotropin-releasing factor subtype 2 suppresses mast cell degranulation and limits the severity of anaphylaxis and stress-induced intestinal permeability. J Allergy Clin Immunol 2019;143:1865–1877.e1864.
15. Fung TC. The microbiota-immune axis as a central mediator of gut-brain communication. Neurobiol Dis 2020;136:104714.
16. Doney E, Cadoret A, Dion-Albert L, Lebel M, Menard C. Inflammation-driven brain and gut barrier dysfunction in stress and mood disorders. Eur J Neurosci 2022;55:2851–2894.
17. Czimmer J, Tache Y. Peripheral Corticotropin Releasing Factor Signaling Inhibits Gastric Emptying: Mechanisms of Action and Role in Stress-related Gastric Alterations of Motor Function. Curr Pharm Des 2017;23:4042–4047.
18. Wang XY, Chen XQ, Wang GQ, et al. A neural circuit for gastric motility disorders driven by gastric dilation in mice. Front Neurosci 2023;17:1069198.
19. Kozakai Y, Hori K, Aye-Mon A, et al. The role of peripheral corticotropin-releasing factor signaling in a rat model of stress-induced gastric hyperalgesia. Biochem Biophys Res Commun 2019;519:797–802.
20. Taché Y, Million M. Role of Corticotropin-releasing Factor Signaling in Stress-related Alterations of Colonic Motility and Hyperalgesia. J Neurogastroenterol Motil 2015;21:8–24.
21. Salvo-Romero E, Martínez C, Lobo B, et al. Overexpression of corticotropin-releasing factor in intestinal mucosal eosinophils is associated with clinical severity in Diarrhea-Predominant Irritable Bowel Syndrome. Sci Rep 2020;10:20706.

22. Ferguson AV, Latchford KJ, Samson WK. The paraventricular nucleus of the hypothalamus - a potential target for integrative treatment of autonomic dysfunction. Expert Opin Ther Targets 2008;12:717–727.
23. Benarroch EE. Paraventricular nucleus, stress response, and cardiovascular disease. Clin Auton Res 2005;15:254–263.
24. Xu JG, Yuan Y, Ma HK, et al. Electroacupuncture ameliorates visceral hypersensitivity and negative emotions by regulating paraventricular hypothalamic nucleus and colonic corticotropin-releasing factor signaling. World J Psychiatry 2025;15:107342.
25. Smart HL, Mayberry JF, Atkinson M. Alternative medicine consultations and remedies in patients with the irritable bowel syndrome. Gut 1986;27:826–828.
26. Bao C, Wu L, Shi Y, et al. Long-term effect of moxibustion on irritable bowel syndrome with diarrhea: a randomized clinical trial. Therap Adv Gastroenterol 2022;15:17562848221075131.
27. Hou YJ, Wang K, Jiang HL, et al. [Study on the mechanism of electroacupuncture repairing intestinal barrier via regulating mast cell in rats with diarrhea-predominant irritable bowel syndrome]. Zhen Ci Yan Jiu 2023;48:281–286.
28. Geng H, Weng SJ, Zhao TT, et al. [Mind-regulating and spleen-strengthening needling technique improves abdominal hypersensitivity and emotion by enhancing functional connectivity between hippocampus and brain regions in diarrhea-predominant irritable bowel syndrome patients]. Zhen Ci Yan Jiu 2021;46:318–325.
29. Xu X, Zheng P, Zhao H, Song B, Wang F. Effect of Electroacupuncture at GV20 on Sleep Deprivation-Induced Depression-Like Behavior in Mice. Evid Based Complement Alternat Med 2020;2020:7481813.
30. Jiang H, Long X, Wang Y, et al. Acupuncture Ameliorates Depression-Like Behaviors Through Modulating the Neuroinflammation Mediated by TLR4 Signaling Pathway in Rats Exposed to Chronic Restraint Stress. Mol Neurobiol 2024;61:2606–2619.
31. Chen Q, Zhang H, Sun CY, et al. Evaluation of two laboratory model methods for diarrheal irritable bowel syndrome. Mol Med 2023;29:5.
32. Al-Chaer ED, Kawasaki M, Pasricha PJ. A new model of chronic visceral hypersensitivity in adult rats induced by colon irritation during postnatal development. Gastroenterology 2000;119:1276–1285.
33. Liu Y, Rao B, Li S, et al. Distinct Hypothalamic Paraventricular Nucleus Inputs to the Cingulate Cortex and Paraventricular Thalamic Nucleus Modulate Anxiety and Arousal. Front Pharmacol 2022;13:814623.
34. Shin A, Staller K, Levinthal DJ. Actionable Clinical Features and Biomarkers to Facilitate the Management of Irritable Bowel Syndrome. Am J Gastroenterol 2025.
35. Ng QX, Soh AYS, Loke W, Lim DY, Yeo WS. The role of inflammation in irritable bowel syndrome (IBS). J Inflamm Res 2018;11:345–349.
36. Nilholm C, Roth B, Ohlsson B. A Dietary Intervention with Reduction of Starch and Sucrose Leads to Reduced Gastrointestinal and Extra-Intestinal Symptoms in IBS Patients. Nutrients 2019;11.

37. Fukudo S. Stress and visceral pain: focusing on irritable bowel syndrome. Pain 2013;154 Suppl 1:S63-s70.
38. Martinez V, Wang L, Million M, Rivier J, Taché Y. Urocortins and the regulation of gastrointestinal motor function and visceral pain. Peptides 2004;25:1733–1744.
39. Larauche M, Kiank C, Tache Y. Corticotropin releasing factor signaling in colon and ileum: regulation by stress and pathophysiological implications. J Physiol Pharmacol 2009;60 Suppl 7:33–46.
40. Taché Y, Martinez V, Wang L, Million M. CRF1 receptor signaling pathways are involved in stress-related alterations of colonic function and viscerosensitivity: implications for irritable bowel syndrome. Br J Pharmacol 2004;141:1321–1330.
41. Larauche M. Novel insights in the role of peripheral corticotropin-releasing factor and mast cells in stress-induced visceral hypersensitivity. Neurogastroenterol Motil 2012;24:201–205.
42. Song Y, Meng QX, Wu K, et al. Disinhibition of PVN-projecting GABAergic neurons in AV region in BNST participates in visceral hypersensitivity in rats. Psychoneuroendocrinology 2020;117:104690.
43. Million M, Wang L, Martinez V, Taché Y. Differential Fos expression in the paraventricular nucleus of the hypothalamus, sacral parasympathetic nucleus and colonic motor response to water avoidance stress in Fischer and Lewis rats. Brain Res 2000;877:345–353.
44. Tache Y, Larauche M, Yuan PQ, Million M. Brain and Gut CRF Signaling: Biological Actions and Role in the Gastrointestinal Tract. Curr Mol Pharmacol 2018;11:51–71.
45. Spencer RL, Deak T. A users guide to HPA axis research. Physiol Behav 2017;178:43–65.
46. Zhang H, Wang Z, Wang G, et al. Understanding the Connection between Gut Homeostasis and Psychological Stress. J Nutr 2023;153:924–939.
47. Tian Y, Yang XW, Chen L, et al. Activation of CRF/CRFR1 Signaling in the Central Nucleus of the Amygdala Contributes to Chronic Stress-Induced Exacerbation of Neuropathic Pain by Enhancing GluN2B-NMDA Receptor-Mediated Synaptic Plasticity in Adult Male Rats. J Pain 2024;25:104495.
48. Vale W, Spiess J, Rivier C, Rivier J. Characterization of a 41-residue ovine hypothalamic peptide that stimulates secretion of corticotropin and beta-endorphin. Science 1981;213:1394–1397.
49. Xu X, Zheng S, Ren J, et al. Hypothalamic CRF neurons facilitate brain reward function. Curr Biol 2024;34:389–402.e385.
50. Binder EB, Nemeroff CB. The CRF system, stress, depression and anxiety-insights from human genetic studies. Mol Psychiatry 2010;15:574–588.
51. Mönnikes H, Schmidt BG, Taché Y. Psychological stress-induced accelerated colonic transit in rats involves hypothalamic corticotropin-releasing factor. Gastroenterology 1993;104:716–723.
52. Saito-Nakaya K, Hasegawa R, Nagura Y, Ito H, Fukudo S. Corticotropin-releasing hormone receptor 1 antagonist blocks colonic hypersensitivity induced by a combination of inflammation and repetitive colorectal distension. Neurogastroenterol Motil 2008;20:1147–1156.
53. Yuan PQ, Wu SV, Wang L, Taché Y. Corticotropin releasing factor in the rat colon: expression, localization and upregulation by endotoxin. Peptides 2010;31:322–331.

54. o'malley D, Julio-Pieper M, Gibney SM, Gosselin RD, Dinan TG, Cryan JF. Differential stress-induced alterations of colonic corticotropin-releasing factor receptors in the Wistar Kyoto rat. Neurogastroenterol Motil 2010;22:301–311.
55. Gourcerol G, Wu SV, Yuan PQ, et al. Activation of corticotropin-releasing factor receptor 2 mediates the colonic motor coping response to acute stress in rodents. Gastroenterology 2011;140:1586–1596.e1586.
56. Kawahito Y, Sano H, Kawata M, et al. Local secretion of corticotropin-releasing hormone by enterochromaffin cells in human colon. Gastroenterology 1994;106:859–865.
57. O'Malley D, Cryan JF, Dinan TG. Crosstalk between interleukin-6 and corticotropin-releasing factor modulate submucosal plexus activity and colonic secretion. Brain Behav Immun 2013;30:115–124.
58. Kimura T, Amano T, Uehara H, et al. Urocortin I is present in the enteric nervous system and exerts an excitatory effect via cholinergic and serotonergic pathways in the rat colon. Am J Physiol Gastrointest Liver Physiol 2007;293:G903-910.
59. Wang SH, Dong L, Luo JY, et al. Decreased expression of serotonin in the jejunum and increased numbers of mast cells in the terminal ileum in patients with irritable bowel syndrome. World J Gastroenterol 2007;13:6041–6047.
60. Overman EL, Rivier JE, Moeser AJ. CRF induces intestinal epithelial barrier injury via the release of mast cell proteases and TNF-α. PLoS One 2012;7:e39935.
61. Lee HS, Lobbestael E, Vermeire S, Sabino J, Cleynen I. Inflammatory bowel disease and Parkinson's disease: common pathophysiological links. Gut 2021;70:408–417.
62. Wallon C, Yang PC, Keita AV, et al. Corticotropin-releasing hormone (CRH) regulates macromolecular permeability via mast cells in normal human colonic biopsies in vitro. Gut 2008;57:50–58.
63. Martin-Viñas JJ, Quigley EM. Immune response in irritable bowel syndrome: A systematic review of systemic and mucosal inflammatory mediators. J Dig Dis 2016;17:572–581.
64. Hasler WL, Grabauskas G, Singh P, Owyang C. Mast cell mediation of visceral sensation and permeability in irritable bowel syndrome. Neurogastroenterol Motil 2022;34:e14339.
65. Mann ER, Lam YK, Uhlig HH. Short-chain fatty acids: linking diet, the microbiome and immunity. Nat Rev Immunol 2024;24:577–595.
66. Berlin F, Mogren S, Tutzauer J, Andersson CK. Mast Cell Proteases Tryptase and Chymase Induce Migratory and Morphological Alterations in Bronchial Epithelial Cells. Int J Mol Sci 2021;22.
67. Krysko O, Korsakova D, Teufelberger A, et al. Differential protease content of mast cells and the processing of IL-33 in Alternaria alternata induced allergic airway inflammation in mice. Front Immunol 2023;14:1040493.
68. Bueno L, Fioramonti J. Protease-activated receptor 2 and gut permeability: a review. Neurogastroenterol Motil 2008;20:580–587.
69. Clark IA. How TNF was recognized as a key mechanism of disease. Cytokine Growth Factor Rev 2007;18:335–343.

70. Tang HY, Chen XQ, Wang H, et al. Acupuncture relieves the visceral pain of diarrhea-predominant irritable bowel syndrome rats by regulating P2X4 expression. Am J Transl Res 2022;14:5563–5573.
71. Gowen R, Gamal A, Di Martino L, McCormick TS, Ghannoum MA. Modulating the Microbiome for Crohn's Disease Treatment. Gastroenterology 2023;164:828–840.
72. Barbara G, Zecchi L, Barbaro R, et al. Mucosal permeability and immune activation as potential therapeutic targets of probiotics in irritable bowel syndrome. J Clin Gastroenterol 2012;46 Suppl:S52-55.
73. Hakl R, Litzman J. [Histamine intolerance]. Vnitr Lek 2023;69:37–40.
74. Han XY, Song XG, Ma WL, et al. Electroacupuncture protects the intestinal mucosal barrier in diarrhea-predominant Irritable Bowel Syndrome rats by regulating the MCs/Tryptase/PAR-2/MLCK pathway. Am J Transl Res 2024;16:781–793.
75. Zhang L, Yu C, Chen B, et al. Modulation of colonic function in irritable bowel syndrome rats by electroacupuncture at ST25 and the neurobiological links between ST25 and the colon. Front Neurosci 2022;16:930489.
76. Zhang H, He W, Hu XF, et al. Electroacupuncture Reduces Visceral Pain Via Cannabinoid CB2 Receptors in a Mouse Model of Inflammatory Bowel Disease. Front Pharmacol 2022;13:861799.
77. Zhu X, Liu Z, Niu W, et al. Effects of electroacupuncture at ST25 and BL25 in a Sennae-induced rat model of diarrhoea-predominant irritable bowel syndrome. Acupunct Med 2017;35:216–223.
78. Ma Q. Somatotopic organization of autonomic reflexes by acupuncture. Curr Opin Neurobiol 2022;76:102602.
79. Liu S, Wang Z, Su Y, et al. A neuroanatomical basis for electroacupuncture to drive the vagal-adrenal axis. Nature 2021;598:641–645.

Figures

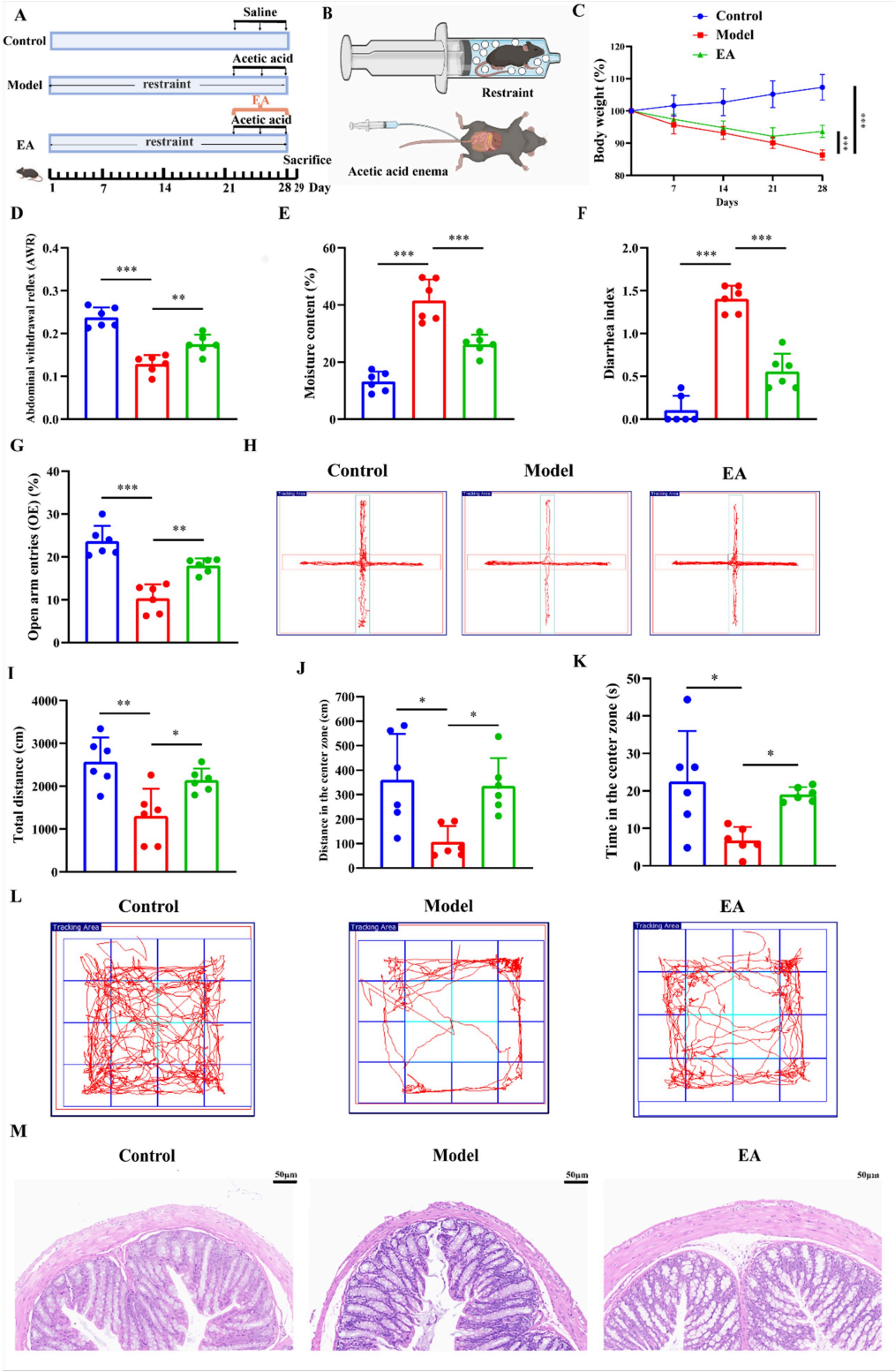


Figure 1

Electroacupuncture alleviates visceral hypersensitivity and anxiety-like behaviors in mice model of IBS-D with emotional comorbidity.

(A) Schematic timeline of the experimental design. (B) Schematic representation of the procedure used to establish the model of IBS-D with emotional comorbidity. (C) Body weight changes monitored throughout the experiment (n=6). (D) Visceral sensitivity assessed by abdominal withdrawal reflex (AWR)

scores in response to graded colorectal distension (CRD) (n=6). (E) Fecal water content (%) (n=6). (F) Diarrhea index scores. (G) Percentage of entries into the open arms in the elevated plus maze (EPM) test (n=6). (H) Representative movement tracking plots for the EPM (n=6). (I–L) Assessment of locomotor activity and anxiety-like behavior in the open field test (OFT) (n=6): (I) total distance traveled; (J) distance traveled in the center zone; (K) time spent in the center zone and (L) representative tracking plots. (M) Representative hematoxylin and eosin (H&E)–stained sections of the distal colon (scale bar: 50 μm) (n=6). Data are presented as mean ± SD. **P*<0.05, ***P*<0.01, ****P*<0.001. (Abbreviations: Control, naive mice; Model, IBS-D with emotional comorbidity mice; *EA, mice receiving electroacupuncture at ST25, BL25, and GV20).*

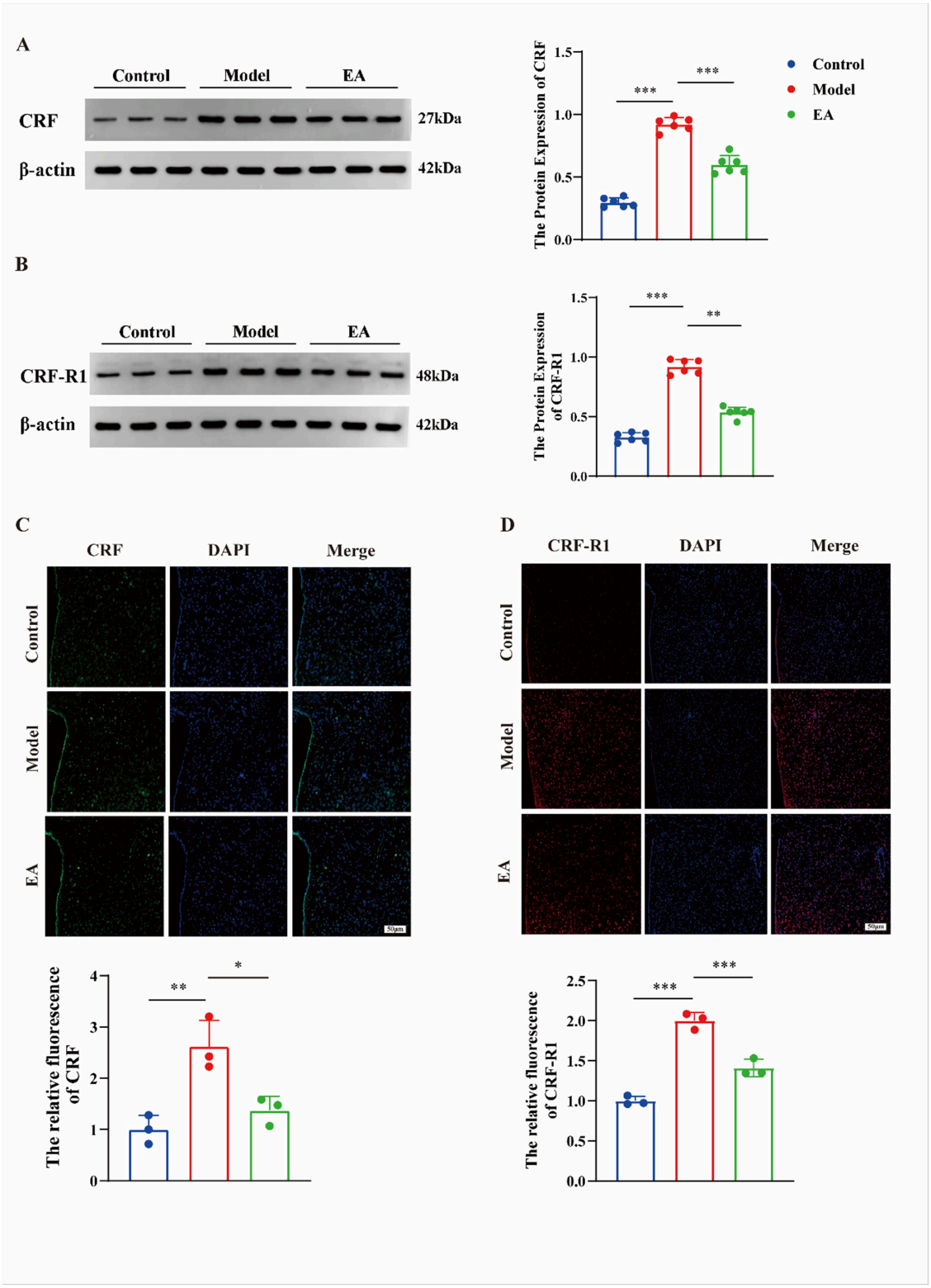


Figure 2

Electroacupuncture suppresses CRF and CRF-R1 protein expression in the hypothalamic PVN of IBS-D mice with emotional comorbidity

(A) Western blot analysis of CRF protein expression in the PVN (n=6). Left: Representative Western blot bands. Right: Densitometric quantification of CRF protein levels normalized to the loading control β-

actin. (B) Western blot analysis of CRF-R1 protein expression in the PVN (n=6). Left: Representative Western blot bands. Right: Densitometric quantification of CRF-R1 protein levels normalized to β-actin. (C) Immunofluorescence assessment of CRF in the PVN (n=3). Up: Representative micrographs showing CRF expression (green). Nuclei were counterstained with DAPI (blue). Bottom: Quantification of the mean fluorescence intensity of CRF. Scale bar: 50 μm. (D) Immunofluorescence assessment of CRF-R1 in the PVN (n=3). Up: Representative micrographs showing CRF-R1 expression (red). Nuclei were counterstained with DAPI (blue). Bottom: Quantification of the mean fluorescence intensity of CRF-R1. Scale bar: 50 μm. Data are presented as mean ± SD. *P<0.05, **P<0.01, ***P<0.001.

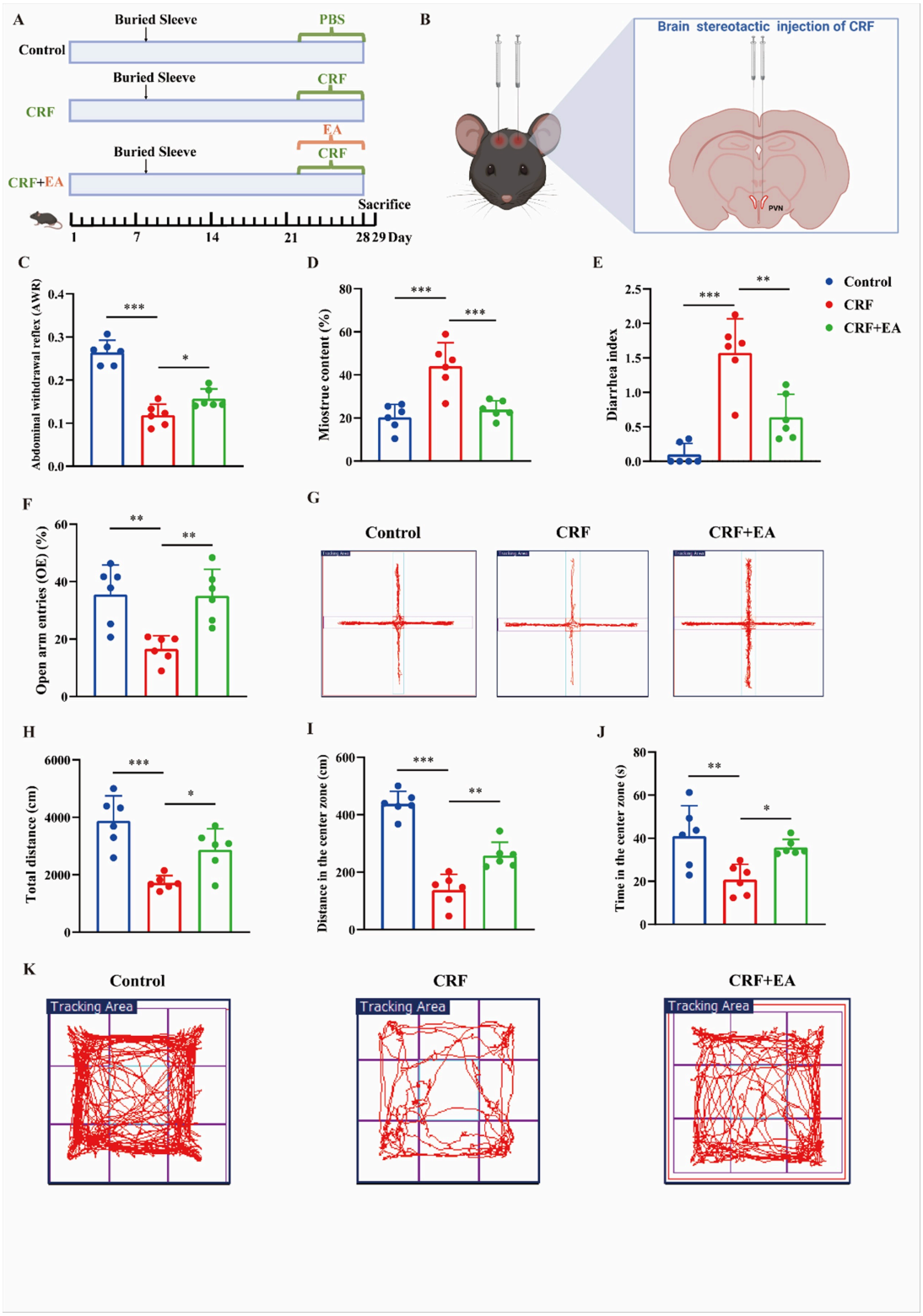


Figure 3

Activation of PVN CRF signaling induces IBS-D-like and anxiety-like phenotypes that are attenuated by electroacupuncture

(A) Schematic timeline of the experimental design. (B) Schematic illustration of bilateral stereotaxic microinjection of CRF (or vehicle) into the PVN. (C)Visceral sensitivity assessed by AWR scores in

response to graded colorectal distension (CRD) (n=6). (D) Fecal water content (%) (n=6). (E) Diarrhea index scores (n=6). (F) Anxiety-like behavior in the elevated plus maze (EPM) (n=6): percentage of entries into the open arms. (G) Representative movement tracking plots for the EPM test corresponding to (F). (H–K) Assessment of locomotor activity and anxiety-like behavior in the open field test (OFT) (n=6): (H) total distance traveled; (I) distance traveled in the center zone; (J) time spent in the center zone; and (K) representative movement tracking plots for the OFT. Data are presented as mean ± SD. **P*<0.05, ***P*<0.01, ****P*<0.001. (Abbreviations: Control, bilateral PVN microinjection of vehicle (PBS); CRF, bilateral PVN microinjection of CRF; CRF+EA, bilateral PVN microinjection of CRF followed by electroacupuncture).

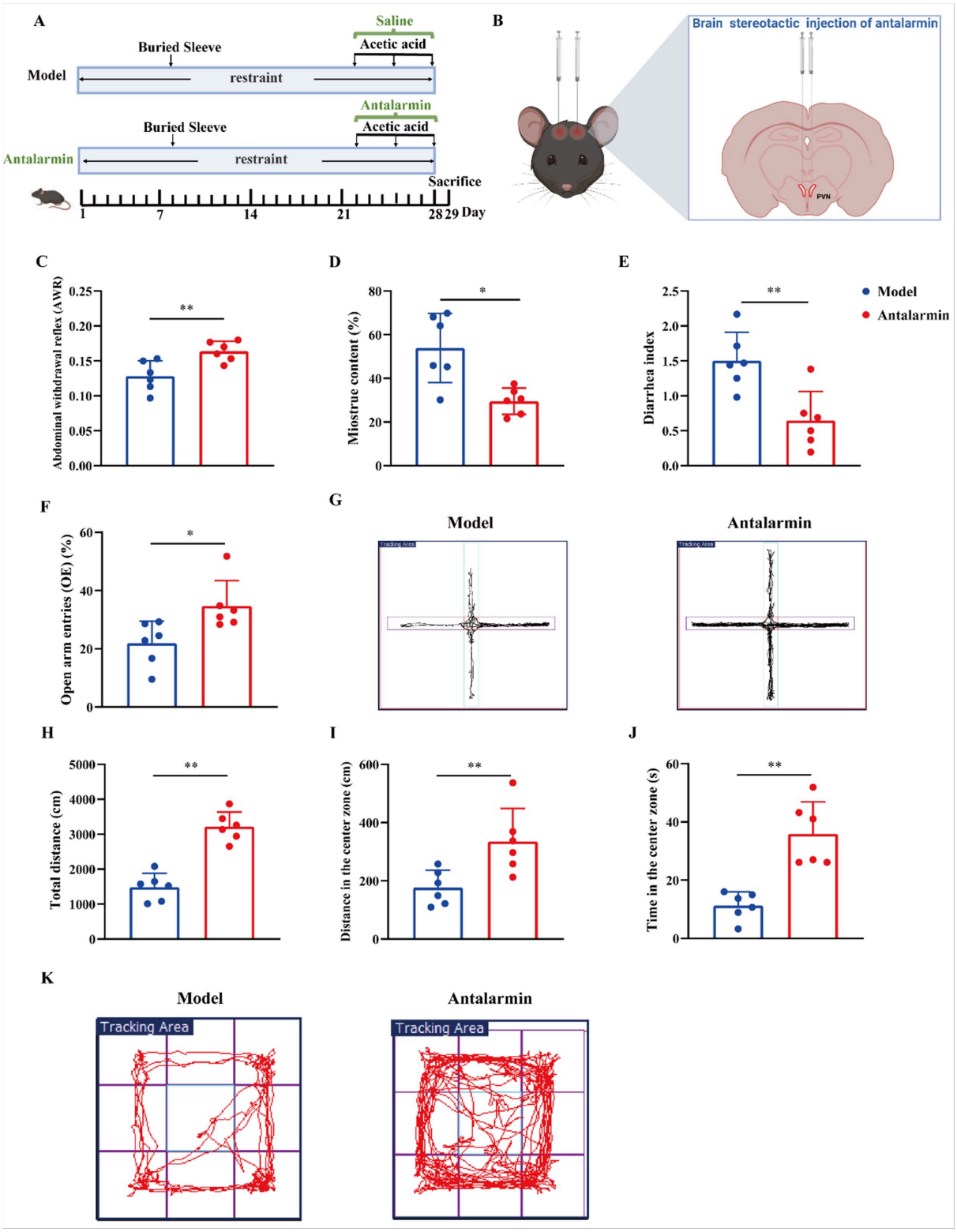


Figure 4

Blockade of PVN CRF-R1 signaling alleviates IBS-D-like and anxiety-like phenotypes in comorbidity model mice

(A) Schematic timeline of the experimental design. (B) Schematic illustration of bilateral stereotaxic microinjection of the CRF-R1 antagonist antalarmin (or vehicle) into the PVN. (C) Visceral sensitivity

assessed by AWR scores in response to graded colorectal distension (CRD) (n=6). (D) Fecal water content (%) (n=6). (E) Diarrhea index scores (n=6). (F) Anxiety-like behavior in the elevated plus maze (EPM) (n=6): percentage of entries into the open arms. (G) Representative movement tracking plots for the EPM test corresponding to (F). (H–K) Assessment of locomotor activity and anxiety-like behavior in the open field test (OFT) (n=6): (H) total distance traveled; (I) distance traveled in the center zone; (J) time spent in the center zone; and (K) representative movement tracking plots for the OFT. Data are presented as mean ± SD. *P<0.05, **P<0.01. (Model, comorbidity mice receiving bilateral PVN microinjection of vehicle (2.5% DMSO in saline); Antalarmin, comorbidity mice receiving bilateral PVN microinjection of antalarmin).

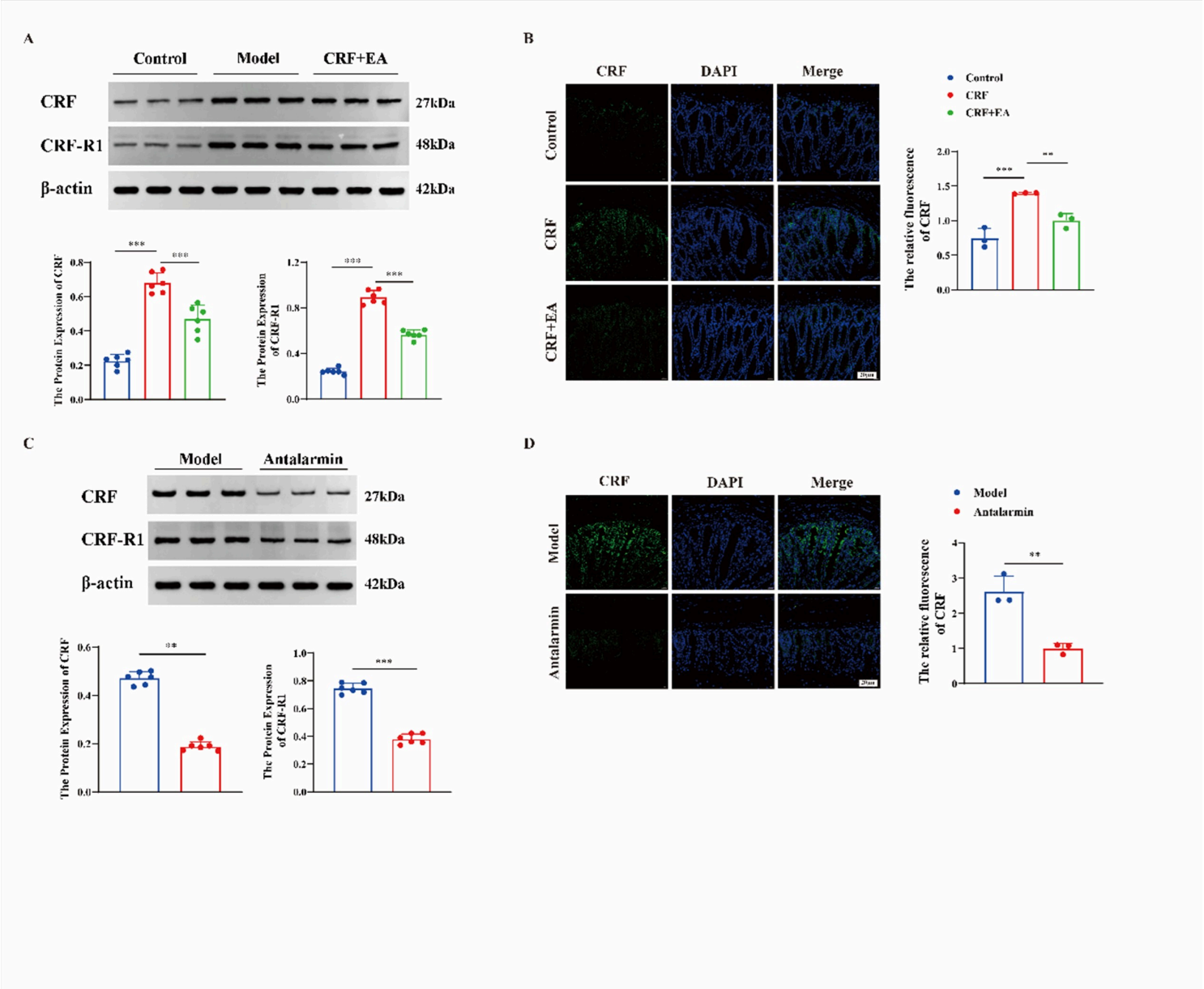


Figure 5

PVN CRF signaling regulates peripheral colonic CRF/CRF-R1 expression

(A) Western blot analysis showing the effects of intra-PVN CRF administration and EA intervention on colonic CRF and CRF-R1 expression (n=6). Top: Representative Western blot bands in distal colon tissues. Bottom: Densitometric quantification of colonic CRF (left) and CRF-R1 (right) protein levels normalized to β-actin. (B) Immunofluorescence analysis of colonic CRF expression after intra-PVN CRF administration and EA intervention (n=3). Left: Representative immunofluorescence micrographs showing CRF expression (green) in the distal colon. Right: Quantification of the mean fluorescence intensity of CRF. (C) Western blot analysis showing the effects of intra-PVN antalarmin administration on colonic CRF and CRF-R1 expression (n=6). Top: Representative Western blot bands in distal colon tissues. Bottom: Densitometric quantification of colonic CRF (left) and CRF-R1 (right) protein levels normalized to β-actin. (D) Immunofluorescence analysis of colonic CRF expression after intra-PVN antalarmin administration (n=3). Top: Representative immunofluorescence images showing CRF expression (green) in the distal colon. Bottom: Quantification of the mean fluorescence intensity of CRF. Scale bar: 20 μm. Data are presented as mean ± SD. $^{**}P<0.01$, $^{***}P<0.001$. (Abbreviations: Control, mice receiving bilateral PVN microinjection of saline [vehicle]; CRF, bilateral PVN microinjection of CRF; CRF+EA, CRF microinjection followed by EA treatment; Model, IBS-D with emotional comorbidity mice receiving bilateral PVN microinjection of vehicle [saline with matched DMSO]; Antalarmin, model mice receiving bilateral PVN microinjection of antalarmin).

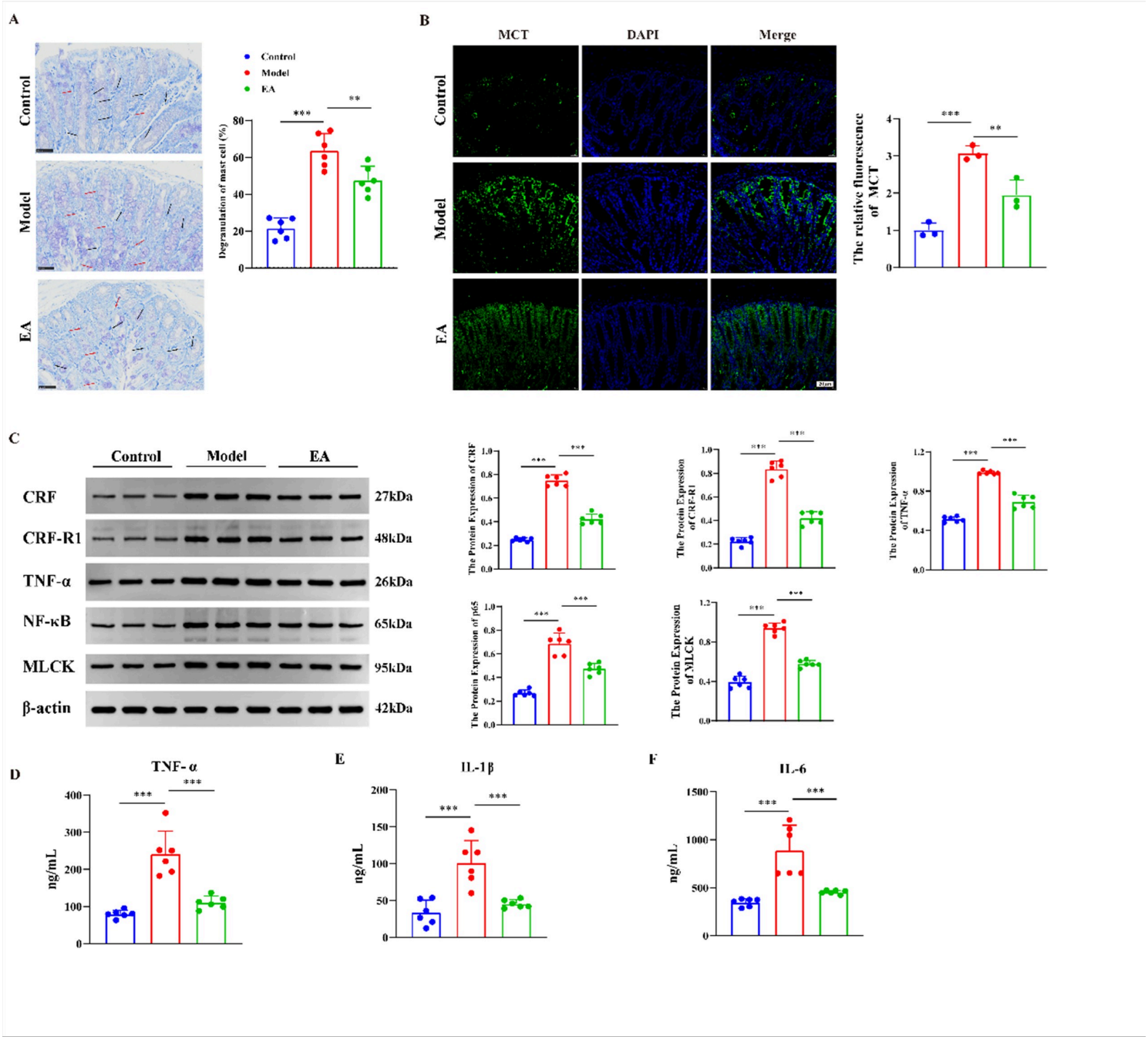


Figure 6

Electroacupuncture attenuates colonic mast cell activation and the downstream TNF-α/NF-κB/MLCK inflammatory pathway

(A) Toluidine blue staining of distal colon sections for the assessment of mast cell degranulation (n=6). Left: Representative micrographs showing mast cell morphology. Black arrows indicate intact mast cells, whereas red arrows indicate degranulated mast cells. Right: Quantification of the mast cell degranulation rate. Scale bar: 50 μm. (B) Immunofluorescence analysis of mast cell tryptase (MCT) in the distal colon (n=3). Left: Representative immunofluorescence micrographs showing MCT expression (green). Nuclei were counterstained with DAPI (blue). Right: Quantification of the mean fluorescence

intensity of MCT. Scale bar: 20 μm. (C) Western blot analysis of key proteins in the CRF–mast cell–inflammation axis in the distal colon (n=6). Left: Representative Western blot bands showing the expression of CRF, CRF-R1, TNF-α, NF-κB p65, and MLCK. Right: Densitometric quantification of protein levels relative to β-actin. (D–F) ELISA analysis of serum inflammatory cytokines (n=6): (D) TNF-α; (E) IL-1β; and (F) IL-6. Data are presented as mean ± SD. ***P*<0.01, ****P*<0.001. (Abbreviations: Control, normal group; Model, IBS-D with emotional comorbidity group; EA, electroacupuncture treatment group).

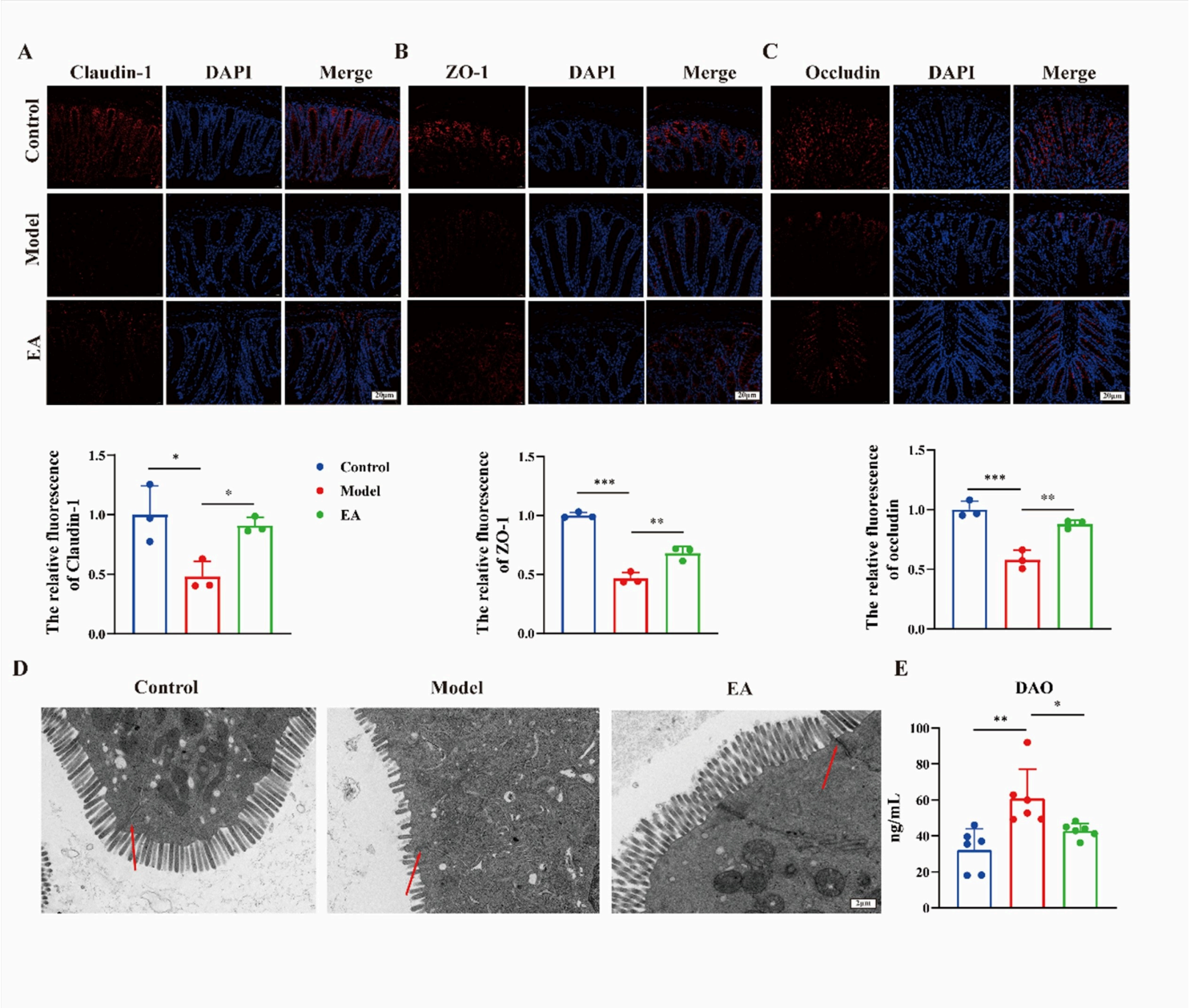


Figure 7

Electroacupuncture restores colonic barrier integrity and ameliorates permeability-related alterations

(A–C) Immunofluorescence analysis of tight junction proteins in the distal colon (n=3). Upper panels: Representative immunofluorescence micrographs showing the expression of (A) Claudin-1, (B) ZO-1, and (C) Occludin (red). Nuclei were counterstained with DAPI (blue). Lower panels: Corresponding

quantification of the mean fluorescence intensity. Scale bar: 20 μm. (D) Representative transmission electron microscopy (TEM) images showing the ultrastructure of epithelial tight junctions in the distal colon. Tight junctions are indicated by red arrows. Compared with the Control group, the Model group showed widened paracellular spaces and reduced electron density, whereas these ultrastructural alterations were attenuated in the EA group. Scale bar: 2 μm. (E) ELISA analysis of serum diamine oxidase (DAO) levels, a marker of intestinal permeability (n=6). Data are presented as mean ± SD. *P<0.05, **P<0.01, ***P<0.001. (Abbreviations: Control, normal group; Model, IBS-D with emotional comorbidity group; EA, electroacupuncture treatment group).

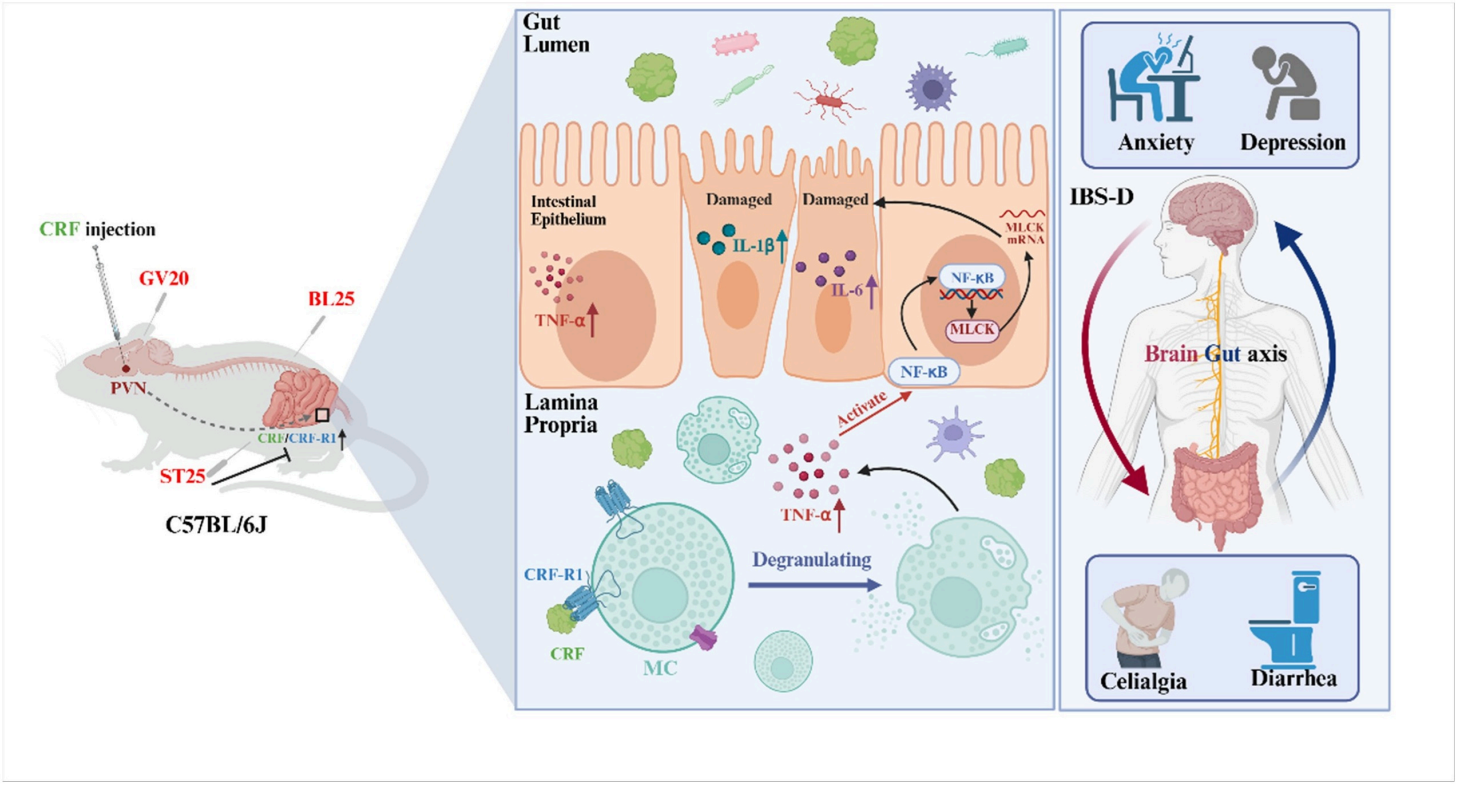


Figure 8

Proposed mechanism by which electroacupuncture ameliorates IBS-D and comorbid anxiety via a PVN-driven brain–gut barrier axis.

Chronic stress induces hyperactivation of CRF neurons in the hypothalamic paraventricular nucleus (PVN), resulting in aberrant CRF/CRF-R1 signaling. This central stress signal propagates to the periphery through the brain–gut axis, upregulating colonic CRF and activating CRF-R1 on mucosal mast cells, thereby promoting mast cell degranulation and the release of pro-inflammatory cytokines (TNF-α, IL-1β, and IL-6). TNF-α activates NF-κB signaling, which increases myosin light-chain kinase (MLCK) expression, leading to tight junction disassembly, epithelial barrier dysfunction, and increased intestinal permeability. These peripheral alterations contribute to visceral hypersensitivity, while persistent PVN CRF overactivation sustains anxiety-like behaviors. Electroacupuncture at ST25, BL25, and GV20

suppresses PVN CRF hyperactivity, attenuates the downstream mast cell–TNF-α–NF-κB–MLCK cascade, restores barrier integrity, and alleviates both visceral and affective abnormalities.

Supplementary Files

This is a list of supplementary files associated with this preprint. Click to download.

- westernblotoriginalreplicates.pdf